Original Article
Activation of A$_{2a}$R attenuates bleomycin-induced pulmonary fibrosis via the SDF-1/CXCR4 axis-related pathway

Yanfan Chen[1*], Xiaoming Yu[2], Yicheng He[3], Lin Zhang[2], Xiaoying Huang[1], Xiaomei Xu[1], Mayun Chen[1], Xiang Chen[1], Liangxing Wang[1*]

[1]Division of Pulmonary Medicine, First Affiliated Hospital of Wenzhou Medical University, Key Laboratory of Heart and Lung, Wenzhou 325000, Zhejiang, China; [2]Division of Pulmonary Medicine, The People's Hospital of Cangnan, Wenzhou Medical University, Cangnan 325800, Zhejiang, China; [3]Institute of Respiratory Disease Zhejiang University, Department of Respiratory Medicine, Second Affiliated Hospital, School of Medicine, Zhejiang University, Hangzhou 310009, China. *Equal contributors.

Abstract: Previous studies in our lab have demonstrated that Adenosine A2a receptor (A$_{2a}$R) gene-knockout mice were vulnerable to pulmonary fibrosis induced by bleomycin (BLM). Inhibition of the SDF-1/CXCR4 axis has been reported to protect the lungs from fibrogenesis in BLM-exposed mice. Little is yet known about the relationships between A$_{2a}$R and the SDF-1/CXCR4 axis in idiopathic pulmonary fibrosis (IPF). This study probes the role of A$_{2a}$R in the fibrotic process and explores the relationship between A$_{2a}$R and the SDF-1/CXCR4 axis in BLM-induced pulmonary fibrosis in mice. In the study, A$_{2a}$R-/- and A$_{2a}$R+/+ BALB/c mice were exposed to BLM by intratracheal instillation, and CGS-21680 (CGS), an A$_{2a}$R agonist, was administered daily for 28 days to the A$_{2a}$R+/+ mice in the BLM-induced fibrosis group. Activation of A$_{2a}$R produced an anti-fibrotic effect as indicated by the evaluations of the lung architecture, microstructure and ultrastructure. The quantitative analysis indicated that treatment with CGS significantly reduced the collagen content in lungs. To explore the potential mechanisms, the expression levels of A$_{2a}$R, SDF-1, and CXCR4 were subsequently determined using ELISA, in situ hybridization (ISH), immunohistochemical staining and western blotting techniques. Administration of CGS markedly suppressed the elevated expression levels of SDF-1 and CXCR4. Moreover, the A$_{2a}$R-/- mice developed more severe pulmonary fibrosis than the normal mice when exposed to BLM. Furthermore, the SDF-1/CXCR4 axis was aberrantly uninhibited in the knockout mice. Together, these findings indicated that A$_{2a}$R alleviated BLM-induced lung fibrosis, at least partially via the SDF-1/CXCR4 pathway, which could be a potential therapeutic target for the treatment of IPF.

Keywords: Idiopathic pulmonary fibrosis, adenosine A2a receptor, stromal cell-derived factor-1, C-X-C chemokine receptor type 4

Introduction

Idiopathic pulmonary fibrosis (IPF) is a devastating and complex disease characterized by the excessive accumulation of extracellular matrix (ECM) and abnormal remodeling of the lung architecture. These features cause progressive dyspnea, wheezing or panting, and finally lead to respiratory failure [1]. The incidence of IPF in the United States ranges from 0.04% to 0.05%, and the five-year survival rate is only 20% [2]. With a median survival of only 2.8 years following diagnosis, IPF represents a very common and fatal condition. To date, the pathogenesis of IPF is incompletely understood and effective treatments are lacking.

Stromal cell derived factor-1 (SDF-1) is a potent chemokine that participates in mobilizing bone marrow-derived stem cells via its receptor, C-X-C chemokine receptor type 4 (CXCR4). The SDF-1/CXCR4 axis has been determined to be important in the complex sequence of events triggered by BLM exposure that culminates in lung repair. Specifically, chronic active injury in the lungs is accompanied by continued expres-

sion of SDF-1 and continued recruitment of CXCR4-expressing stem cells that may be a perpetual reservoir for new fibroblasts [3]. AMD3100, a specific antagonist for CXCR4, directly inhibits the migration of human fibrocytes in response to SDF-1 *in vivo* and reduces the flow of fibrocytes into lungs treated with BLM *in vivo* [4]. These results indicate that the SDF-1/CXCR4 axis plays a key role in the process of pulmonary fibrosis.

Adenosine (Ado) is a crucial endogenously regulated mediator that is broadly expressed in numerous systems of the human body and performs diverse biological functions by binding to various specific receptors that are expressed on the cell surfaces. A_1R, A_{2a}R, A_{2b}R and A_3R are the four known subtypes of Ado receptors. Among these receptors, several experimental studies of A_{2a}R have provided evidence for its multiple protective activities including anti-inflammation [5], anti-oxidation [6] and anti-fibrosis [7]. Previous studies have confirmed that activation of A_{2a}R effectively alleviates renal interstitial fibrosis (RIF) [8], and genetic knockout of A_{2a}R significantly exacerbates the progression of unilateral urethral obstruction (UUO)-induced RIF in mice [9]. Furthermore, we have demonstrated previously that genetic knockout of A_{2a}R significantly exacerbates the progression of pulmonary fibrosis induced by BLM in mice [10]. In addition, the activation of A_{2a}R induces the down-regulation of CXCR4 on CD4+T-cells [11]. However, little work has been done on the correlation between A_{2a}R and SDF-1/CXCR4 axis in the process of pulmonary fibrosis.

The present study aimed to explore the effects of A_{2a}R in a BLM-induced pulmonary fibrosis model by utilizing the A_{2a}RKO mice and to determine whether activation of A_{2a}R would protect the pulmonary system from fibrogenesis by inhibiting the SDF-1/CXCR4 signaling pathway.

Materials and methods

Chemicals and antibodies

Bleomycin (BLM) was purchased from Nippon Kayaku Co., Ltd. (Tokyo, Japan). The A_{2a}R agonist CGS-21680 was obtained from Sigma (St. Louis, MO, USA). A hydroxyproline assay kit was purchased from Nanjing Jiancheng Biochemical Institute (Nanjing, China). The SDF-1 ELISA kit,

the mouse anti-A_{2a}R monoclonal antibody and the rabbit anti-CXCR4 monoclonal antibody were purchased from Abcam (Cambridge, UK). The rabbit anti-SDF-1 polyclonal antibody was purchased from Biorbyt (Cambridge, UK). The rabbit antibody against GAPDH was purchased from CST (Beverly, MA, USA). The horseradish peroxidase-conjugated goat anti-rabbit/mouse immunoglobulin (IgG) was purchased from Boster (Wuhan, China). Rabbit and mouse two-step kits were purchased from ZSGB-BIO (Beijing, China). SuperSignal (R) West Femto Maximum Sensitivity Substrate and a BCA Protein Assay kit were provided by Thermo Fisher Scientific (Waltham, MA, USA). All the other chemicals used in the experiments were commercial products of reagent grade.

Animals

Thirty male BALB/c wild-type (WT) mice and twenty male BALB/c A_{2a}R gene knockout (A_{2a}RKO) mice were acquired from our previously established BALB/c mouse colony [10]. All of the mice were 6 to 8 weeks old and weighed 17-20 g. The mice were provided with free access to food and water and housed in a specific pathogen-free room with a 12:12 h light-dark cycle, controlled room temperature (23±2°C) and humidity (60±10%). All procedures of our experiments were as described in the guide for the Care and Use of Laboratory Animals published by the US National Institute of Health. Our study also adhered to the ARRIVE guidelines.

Establishment of the mouse model of BLM-induced pulmonary fibrosis and experimental design

The animals were randomly divided into five groups (10 animals per group): WT mice control group (WT), WT mice treated with BLM group (WT+BLM), A_{2a}RKO mice control group (A_{2a}RKO), A_{2a}RKO mice treated with BLM group (A_{2a}RKO+BLM), and WT mice treated with BLM and the A_{2a}R agonist (CGS-21680) group (WT+ BLM+CGS). To produce the pulmonary fibrosis models, the mice were intratracheally injected with a single sublethal dose of BLM (5.0 mg/kg), and the control groups received an equal volume of saline (0.9% NaCl). The drug intervention group received intraperitoneal injections of 0.5 mL of CGS (0.25 mg/kg) while the

other groups received 0.5 mL of saline daily for a period of 4 weeks.

Microscopic examination by HE staining and masson-trichrome staining

For microscopic examination, the right lower lobes of the mouse lungs were fixed in 4% para-formaldehyde solution for 24 h, dehydrated in a graded ethanol series, and then embedded in paraffin. Five-micrometer serial sections were stained with hematoxylin-eosin (HE), and the fibrotic pathology was assessed with the Aschcroft scoring system. The collagen deposition, determined by Masson-trichrome staining, was examined in 400× microscopic fields. The blue fibrotic area was quantified as an indicator of the severity of the fibrosis. Image-Pro Plus 6.0 (Media Cybernetics, USA) was used to measure the integrated optical density (IOD) of the positively stained cells.

Ultrastructural examination of interstitial tissues of lung

The samples from the peripheral tissues of the right lower lobes of the lungs were sectioned into small pieces (approximately 1×1×1 mm), fixed with 2.5% glutaraldehyde for more than 2 hours at 4°C and 1% osmium tetroxide for 1 hour, stained with uranyl acetate for 2 hours, dehydrated with acetone, and embedded in EPON 812. The fixed tissues then were cut into ultrathin sections using an LKB-V-type ultramicrotome and examined using a transmission electron microscopy (H-7500, Hitachi, Japan). Images of five randomly selected fields were obtained.

Assessment of lung fibrosis by hydroxyproline (Hyp)

The hydroxyproline content, as an index of the collagen content, was assayed in the lung hydrolysate according to the manufacturer's protocol in the hydroxyproline assay kit manual. Approximately 50-100 mg of lung tissue was hydrolyzed in 1 mL of lysis buffer solution in a water bath at 99°C for 20 min. Following cooling, the absorbance of the colored product was measured at 550 nm using a microplate ELISA analyzer (BIO-RAD, USA) to evaluate collagen deposition. The results were calculated using a standard curve for hydroxyproline.

Detection of SDF-1 in serum using an ELISA

The serum level of SDF-1 was determined using a commercially available ELISA kit according to the manufacturer's instructions. The OD value was determined at 450 nm using a Varioskan LUX Multimode Microplate Reader (Thermo Fisher Scientific Inc., Waltham, MA, USA) and calculated in the linear portion of the curve.

Detection A$_{2a}$R, SDF-1 and CXCR4 protein expression by immunohistochemistry

Five-micrometer sections of the formalin-fixed and paraffin-embedded samples of all lung specimens were prepared. The prepared tissue sections were deparaffinized and rehydrated through a graded alcohol series after being fixed on poly-L-lysine-coated slides overnight at 37°C. Then, they were heated in a microwave oven in 10 mM citrate buffer (pH 6.0) for 3 min. After incubation in a serum-free protein blocking solution for 30 min, the sections were incubated with anti-A$_{2a}$R (diluted 1:200 with PBS), anti-SDF-1 (diluted 1:50 with PBS) or anti-CXCR4 (diluted 1:200 with PBS) antibodies according to the manufacturer's instructions. Horseradish peroxidase-conjugated goat anti-rabbit/mouse IgG was then added. Finally, the sections were counterstained with hematoxylin and mounted. Five different fields at a magnification of 400× were randomly selected for analysis in each section, 8 mice for each group, for a total of 40 fields for each group. The positively stained area (brown) was semi-quantitatively evaluated using Image-Pro Plus 6.0 (Media Cybernetic, Bethesda, MD, USA). The mean values were calculated to show the expression of each protein in each group.

Detection of A$_{2a}$R, SDF-1 and CXCR4 mRNA expression by in situ hybridization

A$_{2a}$R, SDF-1 and CXCR4 mRNAs were measured with an RNAscope FFPE assay kit (Wuhan Boster Biological Technology, Wuhan, Hubei Province, China) according to the manufacturer's instructions. The sequences of the A$_{2a}$R probes were 5'-TGGAA CAACT GCAGT CAGAA AGATG AGAAC TCCAC-3', 5'-CCCCT ACCAG GGGAG CGGAC TCGCT CCACA CTGCA-3' and 5'-CTTAC CCAGG AGCAC CAGGA AGGGC AAGAG CACCC-3'. The sequences of the SDF-1 probes were 5'-AGGTC GTGGT CGTGC TGGTC CTCGT GCTGA-3', 5'-TCAAG CATCT CAAAA TTCTC AAC-
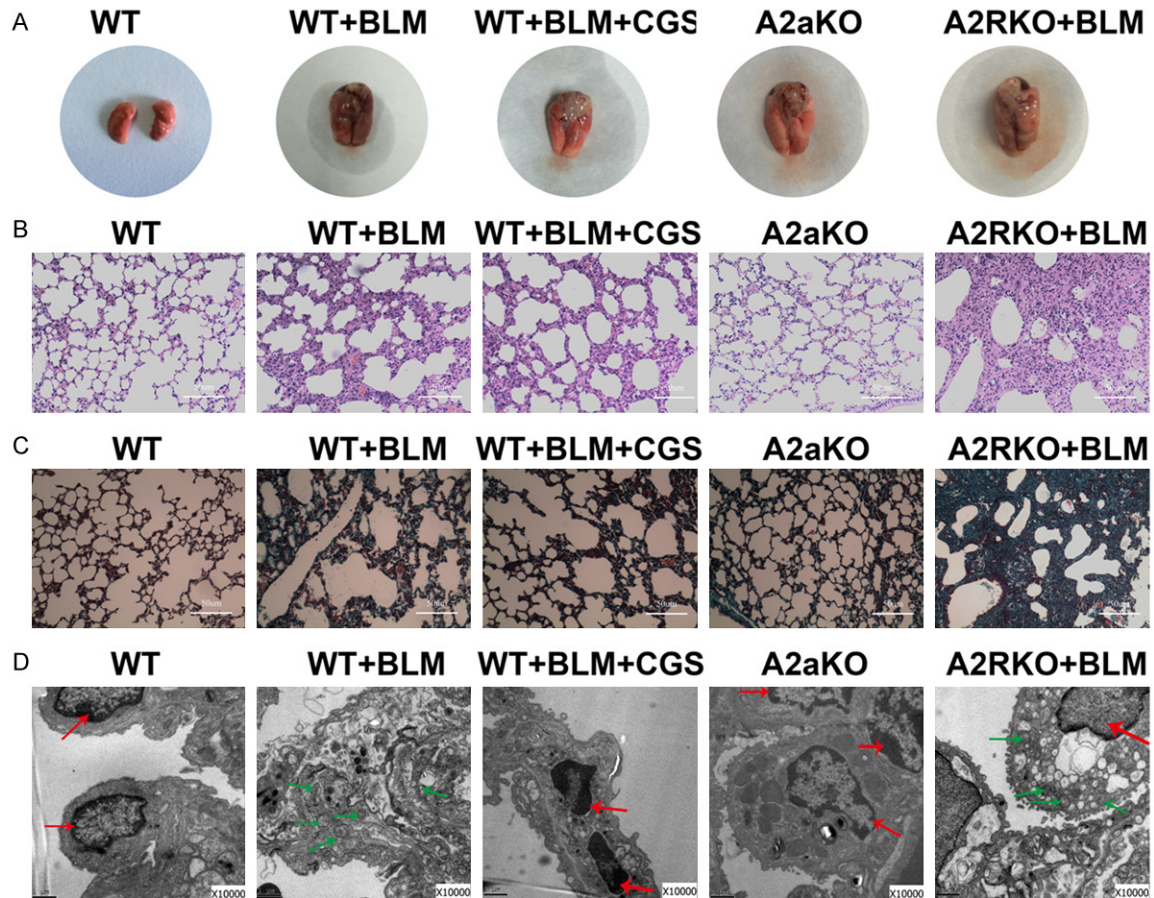
Figure 1. A$_{2a}$R attenuated the BLM-induced pulmonary fibrosis in mice. A. The gross appearance: The lung tissues in the control groups had good elasticity and were red in color, whereas the lung tissues in the BLM-model groups had poor elasticity and were gray in color, not smooth in surface and showed proliferation scars. The effects of BLM on the elasticity and color of lung were reversed in the WT+BLM+CGS group. B. Photomicrographs of lung sections stained with HE (×400). The WT and A$_{2a}$RKO groups showed normal architecture. The WT+BLM and A$_{2a}$RKO+BLM groups showed exaggerated infiltration of inflammatory cells, the loss of normal alveolar structure and extensive thickening of the interalveolar septa. The WT+BLM+CGS group showed ameliorative changes. C. Images of pulmonary tissue sections stained with Masson's trichrome (×400). The collagen is stained blue. The lungs in control groups showed no obvious collagen fiber deposition. The lungs in the model groups displayed abundant collagen deposition. The lungs in the WT+BLM+CGS group exhibited decreased collagen fiber deposition. D. The ultrathin sections of lung tissues in all groups were observed using an H-7500 transmission electron microscope (×10,000). The lungs of the control groups showed little ultrastructural change. The lungs of the model groups displayed destruction of the alveolar epithelial cells and deposition of collagen fibers. The lungs of the WT+BLM+CGS group exhibited improved ultrastructure. Red arrow: cell nucleus; Green arrow: lamellar body.

AC TCCAA-3' and 5'-CAGG AGTA CCTGG AGAAA GCTTT AAACA AG-3'. The sequences of the CXCR4 probes were 5'-GACTA TGACT CCAAC AAGGA ACCCT GCTTC CGGGA-3', 5'-TACCA GAAGA AGCTA AGGAG CATGA CGGAC AAGTA-3' and 5'-GACCG GTACC TCGCT ATTGT CCACG CCACC AACAG-3'. Briefly, 5 μm-thick FFPE lung tissue sections were deparaffinized, digested with pepsin, and hybridized with the probes at 38-42°C overnight. After washing and amplification, the FFPEs were successively incubated

with a biotin-SP-conjugated fraction of a monoclonal mouse anti-digoxin antibody, SASB-POD, and biotin-labeled catalase at room temperature at 37°C for 1 h, 20 min and 20 min, respectively. Finally, the nuclei were counterstained with hematoxylin. The A$_{2a}$R, SDF-1 and CXCR4 mRNA expression levels were examined under a standard bright field microscope at a magnification of 400×. Positive staining was indicated by brown dots in the cytoplasm. The mean value of the IOD in each group was calculated
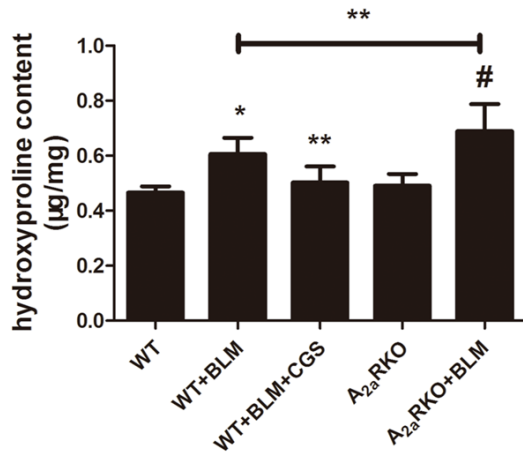
Figure 2. A$_{2a}$R reduced the hyp levels in the mouse model of BLM-induced pulmonary fibrosis. The histogram of hydroxyproline content clearly shows the differences among the groups. The data are expressed as the means ± SD, *: P<0.01 vs. the WT group, #: P<0.01 vs. the A$_{2a}$RKO group, **: P<0.01 vs. the WT+BLM group; n=8.

to display the expression of mRNA using Quantity One-4.6.2 software. Eight sections were randomly selected in each group for analysis. Samples were considered adequate when the UBC mRNA signals were easily visible under a 10× magnification objective lens.

Western blotting analysis

Equal weights (100 mg) of the lung tissues were homogenized in 400 μL ice-cold RIPA lysis buffer containing 1% phenylmethanesulfonyl-fluoride (PMSF) for 30 min. These samples were then subjected to 3 cycles of an ultrasonic cell disruptor for 5 s each time. After lysis for 30 min, the lysates were centrifuged at 12000 rpm for 30 min at 4°C. The protein-containing supernatants were collected, and the protein concentrations were measured with a Pierce BCA Protein Assay kit. After incubation in boiling water for 10 min, the total proteins were denatured for long-time cold storage. Equal amounts of protein (40 μg) were separated on 10% SDS-PAGE gels, transferred to PVDF membranes, blocked with 5% milk, and subsequently incubated with specific primary rabbit antibodies against A$_{2a}$R (1:1000), SDF-1 (1:500), CXCR4 (1:100), or GAPDH (1:5000) at 4°C, overnight. The membranes were incubated with the secondary antibody, an HRP-conjugated goat anti-rabbit IgG (1:10,000) in diluted TBST (1:1000). GAPDH was selected as the control for protein loading differences. Then, the protein bands were detected using electrochemiluminescence (ECL) reagents. Finally, the optical densities of immunoblots were calculated using Quantity One-4.6.2 software (Bio-Rad Laboratories, Hercules, CA, USA).

Statistical analysis

The means ± standard deviation (SD) of the data were computed. The significant differences among the data sets were analyzed using one-way analysis of variance followed by posthoc comparisons using the LSD test (equal variances assumed). Statistical analyses were processed by SPSS (SPSS 17.0, SPSS Inc., Chicago, IL, USA). P-values <0.01 were considered statistically significant.

Results

A$_{2a}$R attenuated BLM-induced pulmonary fibrosis in mice

Figure 1A shows that the lung tissues in the WT and A$_{2a}$RKO groups had good elasticity and were red in color at the organic level. In contrast, the lung tissues in the WT+BLM and A$_{2a}$RKO+BLM groups had poor elasticity and were gray in color, not smooth on surface and even showed proliferation scarring. In the samples of the lungs subjected to intervention with CGS, the gross morphology of the fibrotic lungs indicated good elasticity and a red color similar to the control groups. The histopathological changes in the lung tissues of the mice were evaluated using HE staining. As shown in **Figure 1B**, the BLM-injured lungs displayed thickened alveolar walls, destroyed and disordered alveoli, stenosed or partially collapsed alveolar spaces, fibroplasia and infiltration of inflammatory cells. Compared with the WT+BLM group, the lungs of the animals that had been treated with the A$_{2a}$R agonist CGS-21680 showed significantly reduced infiltration of inflammatory cells, reduced edema, thrombosis and structure destruction, whereas a strongly contrasting trend was observed in the A$_{2a}$RKO+BLM group. Masson's trichrome staining was used to examine the collagen deposition and distribution for the purpose of assessing the fibrosis in lung tissues. As shown in **Figure 1C**, when compared with their respective controls, significant collagen deposition particularly around the bronchus was observed in the BLM-injured lung tis-
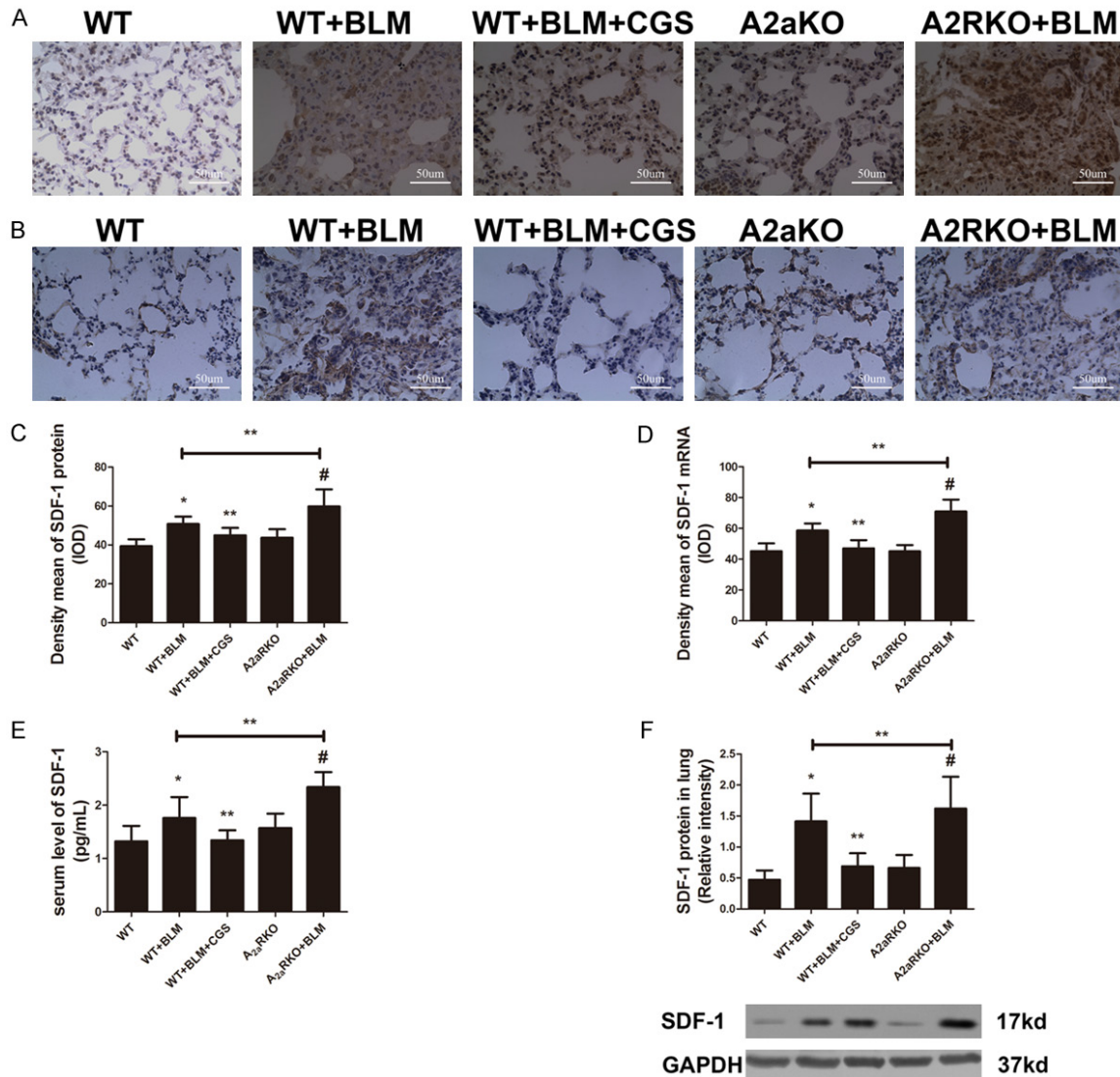
Figure 3. A$_{2a}$R attenuated the expression of SDF-1 in the BLM mouse model. A. Images of SDF-1 immunohistochemistry (×400). B. Images of SDF-1 mRNA in situ hybridization (×400). C. Quantitative analysis of SDF-1 protein by immunohistochemistry. D. Quantitative analysis of SDF-1 mRNA by in situ hybridization. E. Serum levels of SDF-1 by ELISA. F. Images of SDF-1 in lung homogenates detected by WB and quantitative analysis. GAPDH was used as internal control (n=8). The data are expressed as the means ± SD. *: P<0.01 vs. the WT group, #: P<0.01 vs. the A$_{2a}$RKO group, **: P<0.01 vs. the WT+BLM group; n=8.

sues. Compared with the WT+BLM group, the WT+BLM+CGS group showed a significant decrease in collagen deposition. However, the A$_{2a}$RKO+BLM group showed abundant collagen fibers (stained in blue).

Ultrastructural examination was also used to verify the anti-fibrotic effect of A$_{2a}$R activation on BLM-induced lung fibrosis. As shown in **Figure 1D**, the BLM-exposed lungs displayed the following: type I and type II alveolar epithelial cell vacuolation, alveolar septal expansion, collagen fiber hyperplasia, lamellar body cavities, and nuclear condensation. In contrast, the

control groups (WT group and A$_{2a}$RKO group) showed normal lung structure in transmission electron microscopy using a Hitachi H-600 instrument. Compared with the WT+BLM group, CGS treatment alleviated the pulmonary fibrosis whereas the ultrastructural destruction was aggravated in the A$_{2a}$RKO+BLM group.

A$_{2a}$R reduced the hypin the mouse model of BLM-induced pulmonary fibrosis

As one of core index of collagen, the level of hyp in lung tissues was analyzed with a hyp assay kit, which was assessed as the OD value. **Figure**
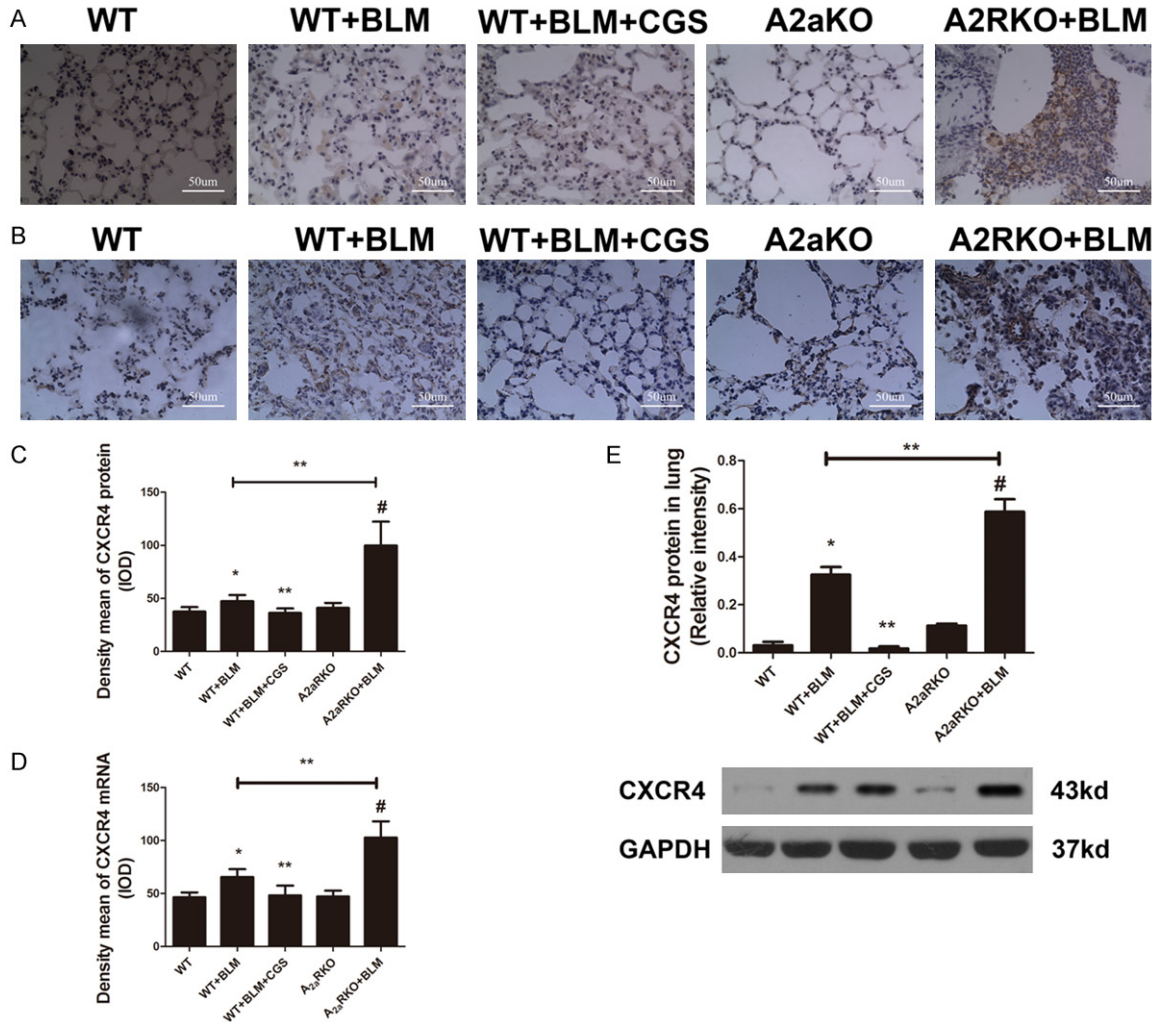
Figure 4. A$_{2a}$R attenuated the expression of CXCR4 in the BLM mouse model. A. Images of CXCR4 immunohisto-chemistry (×400). B. Images of the in situ hybridization for the CXCR4 mRNA (×400). C. Quantitative analysis of the CXCR4 protein by immunohistochemistry. D. Quantitative analysis of the in situ hybridization for the CXCR4 mRNA. E. Images of CXCR4 in the lung homogenates determined using WB and the quantitative analysis. GAPDH was used as an internal control (n=8). The data are expressed as the means ± SD. *: P<0.01 vs. the WT group, #: P<0.01 vs. the A$_{2a}$RKO group, **: P<0.01 vs the WT+BLM group; n=8.

2 shows that the OD value of the BLM-exposed lung tissues was significantly greater than that in control groups (P<0.01). Compared with WT+BLM group, the OD value of WT+BLM+CGS group was significantly decreased (P<0.01). However, the OD value of A$_{2a}$RKO+BLM group was significantly greater (P<0.01) than that of the WT+BLM group.

A$_{2a}$R weakened the pro-inflammatory function of SDF-1/CXCR4 axis

Previous evidence has indicated that A$_{2a}$R has anti-inflammatory and anti-fibrotic effects in

mice that are subjected to BLM-induced pulmonary fibrosis. However, it was not clear whether A$_{2a}$R directly suppresses the inflammation or acts through some other pathway. The following observations suggested the hypothesis that A$_{2a}$R weakened the pro-inflammatory function of SDF-1/CXCR4 axis in the mouse model of BLM-induced pulmonary fibrosis. To test this hypothesis, we performed a series of experiments.

First, the serum level of SDF-1 was determined using ELISA assays in the model groups and control groups. The SDF-1 (**Figure 3E**) was sig-
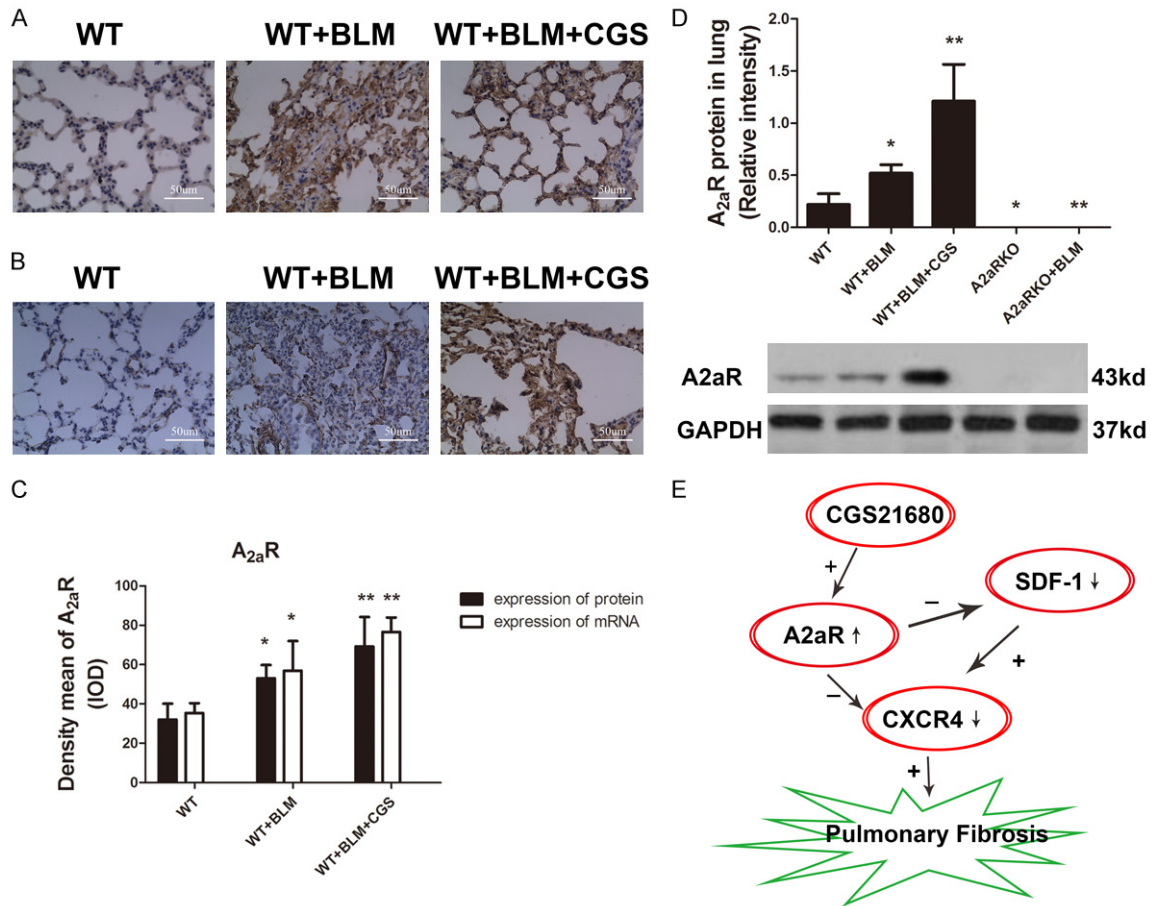
Figure 5. Expression levels of the A_{2a}R protein and mRNA in each group. A. Images of A_{2a}R immunohistochemistry (×400). B. Images of the in situ hybridization for the A_{2a}R mRNA (×400). C. Quantitative analysis of the A_{2a}R protein by immunohistochemistry and the CXCR4 mRNA by in situ hybridization. D. Images of A_{2a}R in lung homogenate determined using WB and quantitative analysis. GAPDH was used as internal control (n=8). E. The signaling pathway that was demonstrated in this study. The data are expressed as the means ± SD. *: P<0.01 vs. the WT group, **: P<0.01 vs. the WT+BLM group; n=8.

nificantly greater in the fibrosis model groups than in the control groups (P<0.01). The SDF-1 was markedly greater in the A_{2a}RKO+BLM group than in the WT+BLM group (P<0.01). However, treatment with CGS appeared to reduce the elevated SDF-1.

Based on the above results, to further clarify the relationship between A_{2a}R and SDF-1/CXCR4 axis, immunohistochemical staining was performed. BLM exposure significantly increased the A_{2a}R, SDF-1 and CXCR4 expression in the mouse lungs versus those of the control group (P<0.01). Treatment with CGS notably decreased the SDF-1 and CXCR4 expression (P<0.01). Compared with the WT group, the two markers were prominently increased in the A_{2a}RKO+BLM group (P<0.01) (**Figures 3A**, **3C**, **4A**, **4C**, **5A** and **5C**).

The mRNA and protein expression levels provided more robust evidence to support the hypothesis described above. In this study, the mRNA expression was determined using in situ hybridization. The mRNA levels of A_{2a}R, SDF-1 and CXCR4 were also notably increased after BLM administration compared to the values in the control group (P<0.01), and treatment with CGS significantly decreased the SDF-1 and CXCR4 mRNA expression in the mouse lungs (P<0.01). In the A_{2a}RKO+BLM group, the SDF-1 and CXCR4 mRNA expression levels were significantly increased compared to those in the WT+BLM group (P<0.01) (**Figures 3B**, **3D**, **4B**, **4D**, **5B** and **5C**).

A similar trend was observed in the protein expression levels assessed using WB. Enhanced protein expression levels of A_{2a}R, SDF-1

and CXCR4 were observed in the BLM-exposed mouse lungs compared to the control group (P<0.01). In the lungs of the mice that were exposed to CGS, the protein levels of SDF-1 and CXCR4 were greatly decreased compared to those in the WT+BLM group (P<0.01). In the mice that lacked the A$_{2a}$R gene, the SDF-1 and CXCR4 proteins were remarkably enhanced compared to those of the control group (P<0.01) (**Figures 3F**, **4E** and **5D**).

Discussion

Our previous study had already demonstrated that deletion of the A$_{2a}$R gene led to exacerbation of the progression of BLM-induced pulmonary fibrosis in mice [10]. In this study, we proved that direct activation of A$_{2a}$R alleviates pulmonary fibrosis and that the potential mechanism might involve down-regulation of the SDF-1/CXCR4 axis.

The pathology of IPF is characterized by apoptosis of the alveolar epithelial cells, repair of fibrosis, and then, destruction of the lung architecture, with the final formation of a honeycomb lung [12]. No animal model has been found so far that exactly mimics the pathological process of human pulmonary fibrosis, but BLM-induced pulmonary fibrosis model has been widely accepted in previous studies. Comparative genomics research has confirmed that mice have a significant advantage as a biological model because the genes of this species are more than 90% homologous to those of humans [13]. Therefore, we established the previously described mouse model of BLM-induced pulmonary fibrosis [14-16]. In the fibrotic mouse models, the increased hyp and the obvious changes observed in the pulmonary histopathology indicated the successful establishment of the IPF model.

Consistent with previous studies [17, 18], our pathologic findings in pulmonary fibrosis included excessive accumulation of ECM and remodeling of the lung architecture. Although the mechanisms remain incompletely clear, both accelerated proliferation or slowed apoptosis of fibroblasts and the excessive ECM accumulation contribute to the development of IPF [17]. Therefore, inhibition of the proliferation of fibroblasts or the secretion of ECM might be efficient therapies for IPF.

A$_{2a}$R, an inhibitory adenosine receptor subtype that is characterized by a high affinity shows physiological effects of inhibiting inflammation and reducing collagen deposition, etc. Recent studies [19-21] have found that the A$_{2a}$R agonist CGS-21680 suppressed the expression of TNF-α. Furthermore, A$_{2a}$R gene knockout mice died due to severe inflammation. In addition, A$_{2a}$R has anti-inflammatory and anti-fibrotic effects in endotoxin-induced liver fibrosis and allergen- or tobacco-induced pneumonia or acute lung injury [22]. In contrast to previous studies, A$_{2a}$R gene knockout mice were examined in the BLM-induced pulmonary fibrosis model in the present study. Using parallel administration of CGS-21680, the study showed more directly and exactly that A$_{2a}$R played a role in the development of pulmonary fibrosis. In this study, BLM exposure resulted in a significantly higher level of hyp in the A$_{2a}$RKO mice than in the WT mice. Compared with the BLM-exposed WT mice, the microstructure and ultrastructure of the lungs was more obviously changed in the BLM-exposed A$_{2a}$RKO mice, which displayed more severe injury of the alveolar epithelial cell as well as greater hyperplasia of the collagen fibers. However, treatment with CGS-21680 not only significantly reduced the content of hyp but also obviously alleviated the fibrosis in the lungs. These results for pulmonary fibrosis are consistent with other reports [8, 9, 23] that A$_{2a}$R activation plays an anti-fibrotic role in renal fibrosis. There are few reports regarding correlations of the function of other adenosine receptors with the SDF-1/CXCR4 axis. However, a study published on May this year reported that inhibition of the SDF-1 receptors CXCR4 and CXCR7 attenuates acute pulmonary inflammation via A2B-receptor signaling [24].

The chemokine SDF-1 plays a functional role in the infiltration, chemotaxis and migration of inflammatory cells. The biological effect of SDF-1 has been described only in the context of its receptor, CXCR4, which is a G-protein coupled seven-transmembrane-domain receptor. Debnath et al. have already found that the SDF-1/CXCR4 axis is involved in the processes of tumorigenesis, HIV-induced pathology, pathological vascular proliferation and pulmonary fibrosis [25]. The statistical analysis in our study showed that the levels of the SDF-1 and CXCR4 genes and proteins were significantly

increased in response to BLM exposure, which confirmed that the SDF-1/CXCR4 axis is involved in the process of pulmonary fibrosis. Subsequently, further study indicated that the application of AMD3100 (a CXCR4 antagonist) significantly alleviates the pulmonary fibrosis [26].

Zhang et al. reported that activation of A$_{2a}$R produces potent anti-inflammatory effects by inducing heterologous desensitization of CXCR4 in dendritic cells [27]. Moreover, activation of A$_{2a}$R could inhibit the aggregation of SDF-1/CXCR4 in the inflammatory response by down-regulating the CXCR4 and CXCR5 receptors on the surfaces of CD4+ lymphocytes [11]. However, much less research has been performed regarding the expression of A$_{2a}$R and its relationship with the SDF-1/CXCR4 axis with respect to the pulmonary fibrosis induced by BLM. The data from our studies indicated that after intervention with the A$_{2a}$R-specific agonist CGS-21680 or when A$_{2a}$R expression was increased, the levels of SDF-1 in serum and SDF-1/CXCR4 in the lung tissues significantly decreased in the mouse model of fibrosis. In addition, the content of hyp and the deposition of collagen fibers decreased, and the damage to the alveolar epithelial cells was significantly reduced. The opposite results were observed in the absence of the A$_{2a}$R gene. Thus, the results of this study consistently showed that activation of A$_{2a}$R suppressed the aberrant activation of SDF-1/CXCR axis in the progression of pulmonary fibrosis (**Figure 5E**).

Conclusions

In summary, activation of A$_{2a}$R is effective in protecting the lung architecture from fibrosis and remodeling partially via a mechanism that involves the attenuation of the chemotactic function of SDF-1/CXCR4 axis. These results provide significant insight into the protective effects of drugs that function by activating A$_{2a}$R in IPF. The underlying mechanisms may become a theoretical basis for strategies for the management of clinical IPF.

Acknowledgements

Disclosure of conflict of interest

None.

Authors' contribution

Associate Prof. Chen YF and Prof. Wang LX contributed to the conception and design of the study, the acquisition, analysis and interpretation of data, and drafting of the manuscript. Dr. Yu XM contributed to the study conception, literature search and the English drafts of the manuscript and figures. Dr. He YC contributed to the study design, completion of the experiments, data acquisition and interpretation of results. The other authors contributed suggestions for improvement of the article. All authors have read and approved the final version of the manuscript. All authors take responsibility for the integrity of the data and accuracy of the data analysis.

Abbreviations

IPF, Idiopathic pulmonary fibrosis; A$_{2a}$R, Adenosine A2a receptor; hyp, hydroxyproline; SDF-1, stromal cell derived factor-1; CXCR4, C-X-C chemokine receptor type 4; Ado, Adenosine.

Address correspondence to: Drs. Yanfan Chen and Liangxing Wang, Division of Pulmonary Medicine, First Affiliated Hospital of Wenzhou Medical University, Key Laboratory of Heart and Lung, Wenzhou 325000, Zhejiang, China. Tel: +8657755579272, +8657786689885; E-mail: chenyf2605@163.com (YFC); wlx@wzmc.net (LXW)

References

[1] Chen X, Zhang X, Li X and Wang Z. Who and what should we rely on in early diagnosis of idiopathic pulmonary fibrosis? Eur Respir J 2013; 41: 249-250.

[2] Raghu G, Collard HR, Egan JJ, Martinez FJ, Behr J, Brown KK, Colby TV, Cordier JF, Flaherty KR, Lasky JA, Lynch DA, Ryu JH, Swigris JJ, Wells AU, Ancochea J, Bouros D, Carvalho C, Costabel U, Ebina M, Hansell DM, Johkoh T, Kim DS, King TE Jr, Kondoh Y, Myers J, Muller NL, Nicholson AG, Richeldi L, Selman M, Dudden RF, Griss BS, Protzko SL, Schunemann HJ; Fibrosis AEJACoIP. An official ATS/ERS/JRS/ALAT statement: idiopathic pulmonary fibrosis:

evidence-based guidelines for diagnosis and management. Am J Respir Crit Care Med 2011; 183: 788-824.

[3] Xu J, Mora A, Shim H, Stecenko A, Brigham KL and Rojas M. Role of the SDF-1/CXCR4 axis in the pathogenesis of lung injury and fibrosis. Am J Respir Cell Mol Biol 2007; 37: 291-299.

[4] Makino H, Aono Y, Azuma M, Kishi M, Yokota Y, Kinoshita K, Takezaki A, Kishi J, Kawano H, Ogawa H, Uehara H, Izumi K, Sone S and Nishioka Y. Antifibrotic effects of CXCR4 antagonist in bleomycin-induced pulmonary fibrosis in mice. J Med Invest 2013; 60: 127-137.

[5] Thiel M, Chouker A, Ohta A, Jackson E, Caldwell C, Smith P, Lukashev D, Bittmann I and Sitkovsky MV. Oxygenation inhibits the physiological tissue-protecting mechanism and thereby exacerbates acute inflammatory lung injury. PLoS Biol 2005; 3: e174.

[6] Zygmunt M, Golembiowska K, Drabczynska A, Kiec-Kononowicz K and Sapa J. Anti-inflammatory, antioxidant, and antiparkinsonian effects of adenosine A2A receptor antagonists. Pharmacol Biochem Behav 2015; 132: 71-78.

[7] Scheibner KA, Boodoo S, Collins S, Black KE, Chan-Li Y, Zarek P, Powell JD and Horton MR. The adenosine a2a receptor inhibits matrix-induced inflammation in a novel fashion. Am J Respir Cell Mol Biol 2009; 40: 251-259.

[8] Xiao H, Shen HY, Liu W, Xiong RP, Li P, Meng G, Yang N, Chen X, Si LY and Zhou YG. Adenosine A2A receptor: a target for regulating renal interstitial fibrosis in obstructive nephropathy. PLoS One 2013; 8: e60173.

[9] Xiao H, Si LY, Liu W, Li N, Meng G, Yang N, Chen X, Zhou YG and Shen HY. The effects of adenosine A2A receptor knockout on renal interstitial fibrosis in a mouse model of unilateral ureteral obstruction. Acta Histochem 2013; 115: 315-319.

[10] Huang X, He Y, Chen Y, Wu P, Gui D, Cai H, Chen A, Chen M, Dai C, Yao D and Wang L. Baicalin attenuates bleomycin-induced pulmonary fibrosis via adenosine A2a receptor related TGF-beta1-induced ERK1/2 signaling pathway. BMC Pulm Med 2016; 16: 132.

[11] By Y, Durand-Gorde JM, Condo J, Lejeune PJ, Fenouillet E, Guieu R and Ruf J. Monoclonal antibody-assisted stimulation of adenosine A2A receptors induces simultaneous downregulation of CXCR4 and CCR5 on CD4+ T-cells. Hum Immunol 2010; 71: 1073-1076.

[12] Plataki M, Koutsopoulos AV, Darivianaki K, Delides G, Siafakas NM and Bouros D. Expression of apoptotic and antiapoptotic markers in epithelial cells in idiopathic pulmonary fibrosis. Chest 2005; 127: 266-274.

[13] Gregory SG, Sekhon M, Schein J, Zhao S, Osoegawa K, Scott CE, Evans RS, Burridge PW, Cox TV, Fox CA, Hutton RD, Mullenger IR, Phil-

lips KJ, Smith J, Stalker J, Threadgold GJ, Birney E, Wylie K, Chinwalla A, Wallis J, Hillier L, Carter J, Gaige T, Jaeger S, Kremitzki C, Layman D, Maas J, McGrane R, Mead K, Walker R, Jones S, Smith M, Asano J, Bosdet I, Chan S, Chittaranjan S, Chiu R, Fjell C, Fuhrmann D, Girn N, Gray C, Guin R, Hsiao L, Krzywinski M, Kutsche R, Lee SS, Mathewson C, McLeavy C, Messervier S, Ness S, Pandoh P, Prabhu AL, Saeedi P, Smailus D, Spence L, Stott J, Taylor S, Terpstra W, Tsai M, Vardy J, Wye N, Yang G, Shatsman S, Ayodeji B, Geer K, Tsegaye G, Shvartsbeyn A, Gebregeorgis E, Krol M, Russell D, Overton L, Malek JA, Holmes M, Heaney M, Shetty J, Feldblyum T, Nierman WC, Catanese JJ, Hubbard T, Waterston RH, Rogers J, de Jong PJ, Fraser CM, Marra M, McPherson JD and Bentley DR. A physical map of the mouse genome. Nature 2002; 418: 743-750.

[14] Wang Z, Guo QY, Zhang XJ, Li X, Li WT, Ma XT and Ma LJ. Corilagin attenuates aerosol bleomycin-induced experimental lung injury. Int J Mol Sci 2014; 15: 9762-9779.

[15] Wei YR, Qiu H, Wu Q, Du YK, Yin ZF, Chen SS, Jin YP, Zhao MM, Wang C, Weng D and Li HP. Establishment of the mouse model of acute exacerbation of idiopathic pulmonary fibrosis. Exp Lung Res 2016; 42: 75-86.

[16] Gou S, Zhu T, Wang W, Xiao M, Wang XC and Chen ZH. Glucagon like peptide-1 attenuates bleomycin-induced pulmonary fibrosis, involving the inactivation of NF-kappaB in mice. Int Immunopharmacol 2014; 22: 498-504.

[17] Todd NW, Luzina IG and Atamas SP. Molecular and cellular mechanisms of pulmonary fibrosis. Fibrogenesis Tissue Repair 2012; 5: 11.

[18] Coward WR, Saini G and Jenkins G. The pathogenesis of idiopathic pulmonary fibrosis. Ther Adv Respir Dis 2010; 4: 367-388.

[19] Mustafa SJ, Morrison RR, Teng B and Pelleg A. Adenosine receptors and the heart: role in regulation of coronary blood flow and cardiac electrophysiology. Handb Exp Pharmacol 2009; 161-188.

[20] Newell EA, Exo JL, Verrier JD, Jackson TC, Gillespie DG, Janesko-Feldman K, Kochanek PM and Jackson EK. 2',3'-cAMP, 3'-AMP, 2'-AMP and adenosine inhibit TNF-alpha and CXCL10 production from activated primary murine microglia via A2A receptors. Brain Res 2015; 1594: 27-35.

[21] Sun WC, Berghaus LJ, Moore JN, Hurley DJ, Vandenplas ML, Thompson R and Linden J. Lipopolysaccharide and TNF-alpha modify adenosine A(2A) receptor expression and function in equine monocytes. Vet Immunol Immunopathol 2010; 135: 289-295.

[22] Collins SL, Black KE, Chan-Li Y, Ahn YH, Cole PA, Powell JD and Horton MR. Hyaluronan fragments promote inflammation by down-regulat-

ing the anti-inflammatory A2a receptor. Am J Respir Cell Mol Biol 2011; 45: 675-683.

[23] Garcia GE, Truong LD, Chen JF, Johnson RJ and Feng L. Adenosine A(2A) receptor activation prevents progressive kidney fibrosis in a model of immune-associated chronic inflammation. Kidney Int 2011; 80: 378-388.

[24] Konrad FM, Meichssner N, Bury A, Ngamsri KC and Reutershan J. Inhibition of SDF-1 receptors CXCR4 and CXCR7 attenuates acute pulmonary inflammation via the adenosine A2B-receptor on blood cells. Cell Death Dis 2017; 8: e2832.

[25] Debnath B, Xu S, Grande F, Garofalo A and Neamati N. Small molecule inhibitors of CXCR4. Theranostics 2013; 3: 47-75.

[26] Song JS, Kang CM, Kang HH, Yoon HK, Kim YK, Kim KH, Moon HS and Park SH. Inhibitory effect of CXC chemokine receptor 4 antagonist AMD3100 on bleomycin induced murine pulmonary fibrosis. Exp Mol Med 2010; 42: 465-472.

[27] Zhang N, Yang D, Dong H, Chen Q, Dimitrova DI, Rogers TJ, Sitkovsky M and Oppenheim JJ. Adenosine A2a receptors induce heterologous desensitization of chemokine receptors. Blood 2006; 108: 38-44.